

## CONFORMATIONAL PARTICULARITIES OF A $\beta$ (25-35) PEPTIDE DETERMINED BY INFRARED SPECTROSCOPY

 Gulyaz Najafova<sup>1\*</sup>,  Gulshen Agaeva<sup>2</sup>,  Zahia Boubegtiten-Fezoua<sup>3</sup>,  
Ana Filipa Santos Seica<sup>3</sup>,  Petra Hellwig<sup>3</sup>

<sup>1</sup>French-Azerbaijani University (UFAZ) under Azerbaijan State Oil and Industry University, Baku, Azerbaijan

<sup>2</sup>Institute for Physical Problems, Baku State University, Baku, Azerbaijan

<sup>3</sup>Laboratoire de Bioélectrochimie et Spectroscopie, Université de Strasbourg CNRS, Strasbourg, France

**Abstract.** The Alzheimer's amyloid- $\beta$  (25-35) peptide retains the toxicity and ability to aggregate of the amyloid- $\beta$ (1-40) peptide. The study of the conformational properties of A $\beta$  (25-35) peptide in its soluble monomeric form can play an essential role in determining the mechanism of oligomerization. In this study, we probed the secondary structure of a soluble A $\beta$  (25-35) peptide in water solution at physiological conditions (pH 7.4). We have used Fourier Transformed Infrared Spectroscopy (FTIR) to examine the secondary structure of this peptide. The amide I bands of A $\beta$  (25-35) obtained from transmission-FTIR spectra consists of one main band at 1658 cm<sup>-1</sup>, at both concentrations used (200  $\mu$ M and 1 mM). This band show us that A $\beta$  (25-35) in aqueous solution was mostly organized into a  $\alpha$ -helical structure (48%). The contribution of the unordered structure was found to be about 12%. The proportion of  $\beta$ -sheet and  $\beta$ -turn structures are slightly lower, 12-15% and 13-14%, respectively for both concentrations. FTIR spectra of the peptide in water solution (100  $\mu$ M) after incubation for 12h showed A $\beta$  peptide conformation is critically dependent on the environmental conditions used.

**Keywords:** Alzheimer's amyloid- $\beta$  (25-35) peptide, FTIR spectroscopy, secondary structure, conformation.

**\*Corresponding Author:** Gulyaz Najafova, French-Azerbaijani University (UFAZ) under Azerbaijan State Oil and Industry University, Baku, Azerbaijan, e-mail: [gulyaz.najafova@ufaz.az](mailto:gulyaz.najafova@ufaz.az)

**Received:** 1 March 2024;

**Accepted:** 19 April 2024;

**Published:** 4 June 2024.

### 1. Introduction

Alzheimer's disease (AD) is one of the most common neurodegenerative disorders and the cause of dementia. The disease is pathologically characterized by the aggregation of two proteins in the brain tissues, namely the amyloid- $\beta$  (A $\beta$ ) and the brain-specific tau protein. There is cumulative evidence that A $\beta$  peptides self-assembly into soluble oligomers and insoluble fibrils (Zhao *et al.*, 2014).

The truncated variants of A $\beta$  (1-42) can be directly neurotoxic, inducing oxidative stress and an inflammatory response (Sultana *et al.*, 2006). These events might be

#### How to cite (APA):

Najafova, G.Z., Agaeva, G.A., Boubegtiten-Fezoua, Z., Seica, A.F.S. & Hellwig, P. (2024). Conformational particularities of A $\beta$ (25-35) peptide determined by infrared spectroscopy. *Advanced Physical Research*, 6(2), 73-82 <https://doi.org/10.62476/apr62.73>

mediated by the direct interaction of A $\beta$  aggregates with cellular membranes or by the binding of A $\beta$  to neuronal cellular receptors. A particular fragment, A $\beta$  (25-35) (with sequence GSNKGAIIGLM) is considered to be the functional domain of A $\beta$ , responsible for its neurotoxic properties (Limón *et al.*, 2009) and the biologically active region of A $\beta$  (D'Errico *et al.*, 2008). The A $\beta$  (25-35) peptide possesses many of the characteristics of the full-length A $\beta$  (1-40/42), including its amphiphilic nature and the tendency to aggregate. Its presence in vivo was only recently proven, but the toxicity of fibrillary A $\beta$  (25-35) towards neuronal cells in vitro was previously demonstrated (Resende *et al.*, 2007). There is also evidence that the monomeric form of this peptide may itself be cytotoxic (Clementieta *et al.*, 2005).

The mechanism of the amyloid peptide's toxicity remains unexplained. Several studies demonstrated that the extracellular soluble species of A $\beta$ -peptides (monomers and oligomers) as well as fibrils play a major role in cytotoxicity (Resende *et al.*, 2007; Clementieta *et al.*, 2005). Nevertheless, many important details about soluble A $\beta$  including its structures are missing or contradicting each other. Hence, the study of the conformational properties of A $\beta$  (25-35) peptide in its soluble monomeric form can play an essential role in determining the nature of the earlier species before oligomerization.

Several studies aimed at probing the membrane mediated structure of amyloid peptide A $\beta$  (25-35) to clarify the structure-function relationships of the peptide (Kohno *et al.*, 1996; Coles *et al.*, 1998). Several studies identified the solution conformation of the A $\beta$  (25-35) peptide using hydrophobic solvents such as trifluoroethanol (TFE) and hexafluoroisopropanol (HFIP). For example, CD (circular dichroism) studies found that A $\beta$  (25-35) adopts an ordered conformation including some  $\alpha$ -helix, with the increase of the trifluoroethanol concentration (El-Agnaf *et al.*, 1998) or unordered structures in methanol (Shanmugam & Jayakumar, 2004). In another study using vibrational circular dichroism spectroscopy, A $\beta$  (25-35) in DMSO solution was shown to adopt a  $\beta$ -turn structure (Shanmugam & Polavarapu, 2004). In addition, the three dimensional structure of A $\beta$  (25-35) was determined by NMR (nuclear magnetic resonance) and it was shown that in a solution containing HFIP/water (20/80 v/v) the peptide has a less regular folding in the C-terminal region of the peptide with a  $\beta$ -turns in the 25-28 segment (D'Ursi *et al.*, 2004). A different NMR study have been shown that A $\beta$  (25-35) adopts a *turn-helical structure* in solution containing at least 50% HFIP. This *structure* has a partially ordered turn in the N-terminus (residues 26-28), followed by an  $\alpha$ -helix from residues 28-31 and a  $3_{10}$ -helix spanning the C-terminus residues 32-34 (Wei & Shea, 2006). While in a solution containing 50% TFE was found that Ala<sup>30</sup> to Met<sup>35</sup> in the A $\beta$  (25-35) structure adopts an  $\alpha$ -helical conformation (Lee & Kim, 2004).

Efforts at characterizing the A $\beta$  (25-35) conformation in aqueous solvents have been performed (Wei & Shea, 2006; Millucci *et al.*, 2010; Ma & Nussinov, 2006; Terzi *et al.*, 1994; Song *et al.*, 2018). Simulation using replica exchange molecular dynamics approach revealed that in explicit water the peptide adopts a collapsed coil and to a lesser extent  $\beta$ -hairpin conformation (Wei & Shea, 2006). While the energy landscape calculations show that the extended conformation, together with the  $\alpha$ -helix are important intermediates for A $\beta$  (25-35) peptide oligomerization leading to amyloid formation (Ma & Nussinov, 2006). In addition, the secondary structure of the peptide in buffer solution at pH 4.0 or 5.5 determined by circular dichroism spectroscopy, showed predominantly random coil structure at low peptide concentration (< 125  $\mu$ M) and a  $\beta$ -

sheet structure at higher concentrations (Terzi *et al.*, 1994). However, at pH 7.4 only a  $\beta$ -sheet structure was observed for the peptide even at low concentration (Terzi *et al.*, 1994). Another CD study of the peptide in aqueous solutions (100  $\mu$ M) suggested the presence of unordered structure in water solution and  $\beta$ -sheet structure in phosphate buffer at pH 7.15 (Song *et al.*, 2018). In contrast, when the measurements were performed by ATR-FTIR spectroscopy with the same diluted peptide sample in pure water or buffer solution, aggregated  $\beta$ -sheet structure was observed (Song *et al.*, 2018). Hence, the conformations adopted by the A $\beta$  (25-35) peptide in solution are extremely sensitive to the techniques and the experimental conditions involved.

In this study, we probed the structure of a soluble A $\beta$  (25-35) peptide in water solution at physiological conditions (pH 7.4). We also have used Fourier Transformed Infrared Spectroscopy (FTIR) to examine the secondary structure of the peptide. Our results reveal for the first time that A $\beta$  (25-35) adopts  $\alpha$ -helical conformation in water at pH 7.4. This finding is consistent with the hypothesis that the helix-containing conformer is an important intermediate in A $\beta$  fibril assembly (Fezoui & Teplow, 2002; Kirkitadze *et al.*, 2001; Vivekanandan *et al.*, 2011). The possible role of  $\alpha$ -helical structure in initiating aggregation of the A $\beta$  peptide will be discussed.

## 2. Materials and Methods

### 2.1. Peptide sample preparation

The A $\beta$  (25-35) peptide (GSNKGAIIGLM) was purchased from GeneCust peptides synthesis. We used here a commercially available HCl salt form of A $\beta$  (25-35) peptide (without TFA). The purity of the peptide was estimated to be higher than 95% according to mass spectrometry and HPLC control data provided by GeneCust.

The solubilization procedure for the A $\beta$  (25-35) peptide was adapted from (Song *et al.*, 2018). The peptide (0.5 mg) was dissolved in 500  $\mu$ L of 1,1,1,3,3,3-hexafluoro-2-propanol (HFIP, Sigma Aldrich, France) and subsequently sonicated and vortexed three times for 10 seconds. To ensure complete solubilization of the peptide, the solution was kept in a thermomixer (IsoTherm-System 3880, Eppendorf, Germany) for 24 h at 350 rpm min<sup>-1</sup> at 25°C. After that, the HFIP solvent was removed by a stream of argon and the peptide film was stored in a vacuum drying lyophilizateur (Cosmos model, Cryotec, France) for 24 h. The obtained peptide film was dissolved in deuterium oxide (D<sub>2</sub>O solution with 100 atoms % D, Acros Organics, USA) for a final concentration of 200  $\mu$ M and 1 mM at pD 7.4. Finally, the fresh peptide solutions were stirred 5 min before the FTIR measurements.

### 2.2. Fourier Transformed Infrared Spectroscopy (FTIR)

The infrared spectra were obtained with a Vertex 70 FTIR spectrometer (Bruker, Germany) equipped with a liquid nitrogen MCT (mercury cadmium telluride) detector. The spectrometer was purged with dry air to avoid the contributions from humidity. The FTIR spectra of the peptide obtained in the transmission and in attenuated total reflection (ATR) mode, were recorded in the spectral range from 4000 to 1000 cm<sup>-1</sup> with a scan velocity of 40 kHz. Three spectra with a resolution of 4 cm<sup>-1</sup> (256 co-added scans) were averaged for each peptide sample (200  $\mu$ M or 1 mM). Also, two infrared experiments (transmission or ATR) were performed for each peptide sample. A

reference spectrum was collected for a pure D<sub>2</sub>O and subtracted from the transmission or the ATR-FTIR spectra of the peptide, respectively.

The infrared transmission spectra of the A $\beta$  (25-35) peptide were obtained with a transmission cell made of two calcium fluoride (CaF<sub>2</sub>) windows. 0.5  $\mu$ L of the peptide solution (200  $\mu$ M or 1 mM) were deposited on a window that was covered with a second window. A defined path (17  $\mu$ m) was obtained as described by Barth & Zscherp (2002). The windows were placed in the metallic support and then the transmission cell was placed on the optical path of the IR beam. For ATR-FTIR spectra of the peptide, 2.5  $\mu$ L of the peptide solution (200  $\mu$ M or 1 mM) were deposited on the diamond crystal (Harrick) and the spectra were recorded before obtaining the dry film peptide.

### 2.3. Analysis of the infrared data

Before analysis, a pure D<sub>2</sub>O spectrum was subtracted from the peptide sample spectrum (transmission or ATR-FTIR) in the spectral range from 1800 to 1400  $\text{cm}^{-1}$ . A linear baseline was then subtracted from all spectra. For clarity, the maximum area for the amide I band (1700-1600  $\text{cm}^{-1}$ ) for all spectra shown has been normalized to the same value. The resulting amide I bands were analyzed with an algorithm based on a second-derivative function (Origin Pro 8.5, OriginLab Corporation) and a self-deconvolution procedure (Origin Pro 8.5, OriginLab Corporation) to determine the number and wavenumber of individual bands within the spectral range 1700-1600  $\text{cm}^{-1}$ . The amide I band of each spectrum could be fitted by four bands assigned to the vibration of amide I involved in four different secondary structures.

The Gaussian band profile was used to fit all the individual amide I band components obtained at 1623, 1640, 1658 and 1676  $\text{cm}^{-1}$  and have been assigned to the secondary structure elements in D<sub>2</sub>O as follows:  $\alpha$ -helices (1658  $\text{cm}^{-1}$ ), unordered structures (1640  $\text{cm}^{-1}$ ),  $\beta$ -sheet (1623  $\text{cm}^{-1}$ ) and  $\beta$ -turns (1676  $\text{cm}^{-1}$ ). The relative contributions of the different bands were determined from the fit results obtained for the amide I bands. The amount of each secondary-structure element is given as a percentage and is calculated by dividing the area of one amide I band component by the total area of all amide I band components. The absolute error due to the deconvolution variability and the baseline correction was estimated to be about  $\pm 5\%$ .

## 3. Results

### 3.1. Identification of the secondary structure of A $\beta$ (25-35) by FTIR spectroscopy

The Fourier-transform infrared spectroscopy is an established tool for the characterization of the aggregates formed during the aggregation process of the Alzheimer's amyloid- $\beta$  peptides, A $\beta$  42 (Cerf *et al.*, 2009) and A $\beta$  40 (McLaurin *et al.*, 1999). A full analysis of the protein or the peptide structure requires a complete study of the amide I band (1600-1700  $\text{cm}^{-1}$ ) by curve-fitting (Cerf *et al.*, 2009; Hashioka *et al.*, 2005). In this study, we carried out the deconvolutions of the amide I band obtained for the A $\beta$  (25-35) peptide in aqueous D<sub>2</sub>O solution (pD 7.4) at both concentrations (200  $\mu$ M and 1 mM) (procedure described in Materials and Methods part).

The experiments with the sample at 1 mM were performed to exclude an effect of the concentration on the peptide structure. The transmission and ATR-FTIR spectra in the amide I range could be fitted with 4 components at 1623, 1640, 1658 and 1676  $\text{cm}^{-1}$ .

We assigned individual amide I band components to various elements of peptide secondary structures based on a large body of experimental data (Pike *et al.*, 1993). The assignments of each component and the relative contribution of each structural element in A $\beta$  (25-35) peptide is presented in Tables 1 and 2.

**Table 1.** Comparison of secondary structure composition of A $\beta$  (25-35) peptide in solution in D<sub>2</sub>O

Secondary Structure (%)	Experimental (200 $\mu$ M)	Experimental (1 mM)
$\alpha$ -helices	48	48
Unordered	23	28
$\beta$ -sheets	15	12
$\beta$ -turns	14	13

(pD 7.4) at 200  $\mu$ M and 1 mM obtained from curve fitting of transmission-FTIR spectra

**Table 2.** Comparison of secondary structure composition of A $\beta$  (25-35) peptide in solution in D<sub>2</sub>O

Secondary Structure (%)	Experimental (200 $\mu$ M)	Experimental (1 mM)
$\alpha$ -helices	45	48
Unordered	23	24
$\beta$ -sheets	11	16
$\beta$ -turns	11	12

(pD 7.4) at 200  $\mu$ M and 1 mM obtained from curve fitting of ATR-FTIR spectra

The amide I bands of A $\beta$  (25-35) obtained from transmission-FTIR spectra consists of one main band at 1658 cm<sup>-1</sup>, at both concentrations used (200  $\mu$ M and 1 mM) (Figure 2 A and B). This band show us that A $\beta$  (25-35) in aqueous solution was mostly organized into a  $\alpha$ -helical structure (48%), a value that is consistent with the molecular simulation data presented above (48%) (Table 1). The contribution of the unordered structure was found to be about 12% (Table 1). The proportion of  $\beta$ -sheet and  $\beta$ -turn structures are slightly lower (12-15% and 13-14%, respectively for both concentrations) as compared to the theoretical values (20 % for  $\beta$ -sheet, 20 % for  $\beta$ -turns) (Table 1).

The peptide was measured in both in solution (transmission mode) and before obtaining the dry film (in the ATR mode). This later method allows to distinguish different amyloid aggregated forms (Cerf *et al.*, 2009; Sarroukh *et al.*, 2011; Berthelot *et al.*, 2009). Figure 2 A-B and Table 2 show the direct comparison of 200  $\mu$ M and 1 mM peptide solutions measured by ATR infrared spectroscopy. In both concentrations,

the contributions from  $\alpha$ -helices, unordered,  $\beta$ -sheet and  $\beta$ -turns in the secondary structure of the peptide were highly comparable with the transmission infrared data (Figure 1 and Table 1).

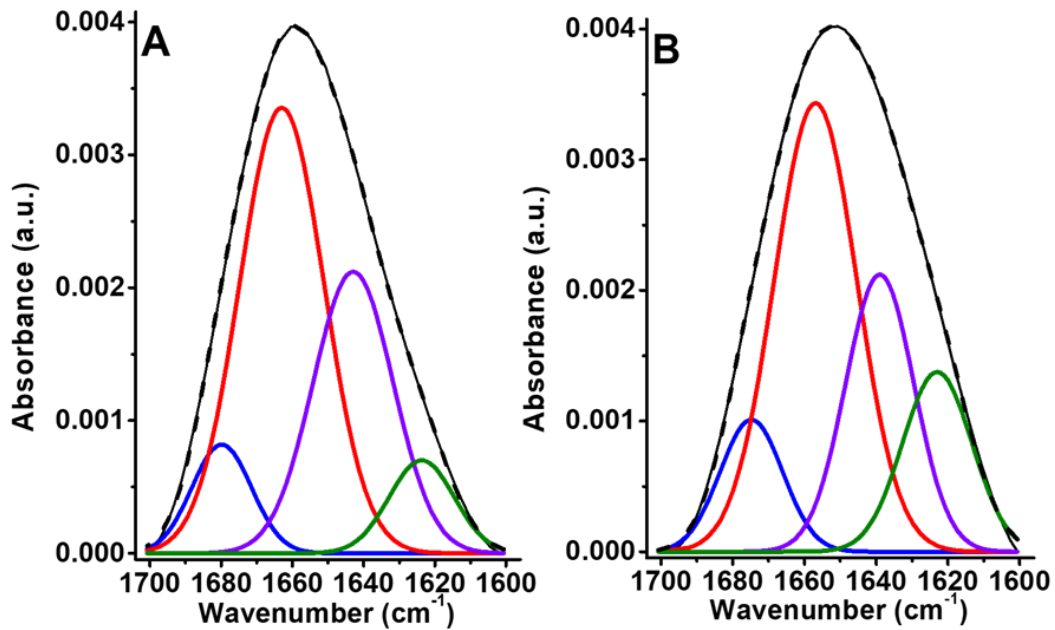


**Figure 1.** Secondary structure analysis of the peptide A $\beta$  (25-35) solution in D<sub>2</sub>O (pD 7.4) at 200 $\mu$ M (A) and 1 mM (B). Curve-fitting of the deconvoluted amide I bands (1700-1600 cm<sup>-1</sup>) obtained from spectra of Transmission-FTIR. The Gaussian curves underneath the experimental curve represent the various secondary structures of the amide I band:  $\alpha$ -helix (red curve), unordered structures (violet curve),  $\beta$ -turns (blue curve) and  $\beta$ -sheets (green curve)

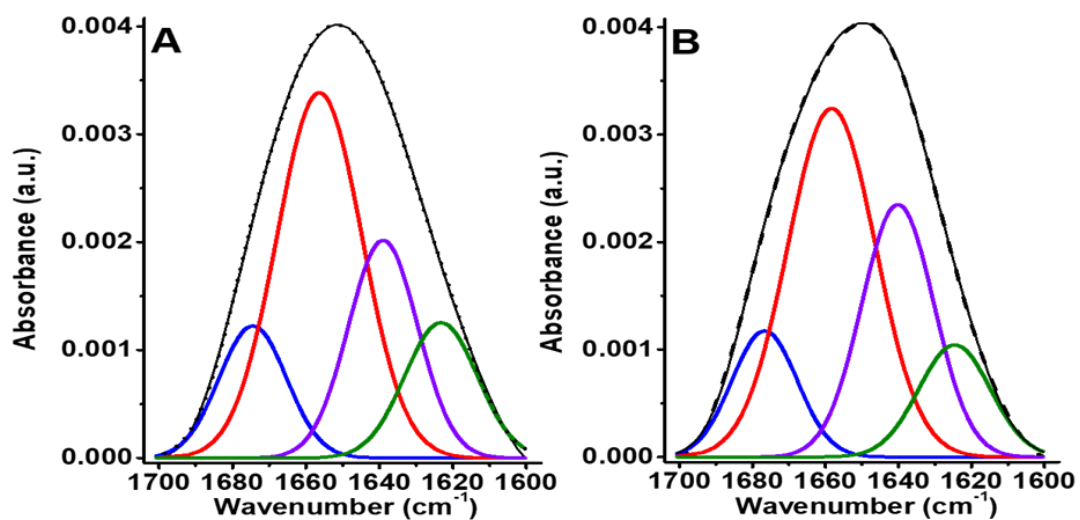


**Figure 2.** Secondary structure analysis of the peptide A $\beta$  (25-35) solution in D<sub>2</sub>O (pD 7.4) at 200 $\mu$ M (A) and 1 mM (B). Curve-fitting of the deconvoluted amide I bands (1700-1600 cm<sup>-1</sup>) obtained from spectra of ATR-FTIR. The Gaussian curves underneath the experimental curve represent the various secondary structures of the amide I band:  $\alpha$ -helix (red curve), unordered structures (violet curve),  $\beta$ -turns (blue curve) and  $\beta$ -sheets (green curve)

#### 4. Discussion

Several studies have shown that the soluble A $\beta$  and Alzheimer's disease are intertwined and that soluble A $\beta$  peptide contributes to disease development and progression (Sarroukh *et al.*, 2013). It is thus crucial to determine the soluble monomeric conformation of the A $\beta$  (25-35) peptide as it can play an important role in determining the nature of early aggregates and the resulting morphology of the amyloid fibril (Celej *et al.*, 2012). Few works have been performed in studying the conformational properties of A $\beta$  (25-35) in aqueous solution, however no consensus is reached so far to describe the soluble peptide structure (Wei & Shea, 2006; Millucci *et al.*, 2010; Ma & Nussinov, 2006; Terzi *et al.*, 1994; Song *et al.*, 2018).

In this work, we obtained the spectroscopic approaches and clearly showed that A $\beta$  (25-35) adopts mostly an  $\alpha$ -helical structure and some smaller contributions of unordered,  $\beta$ -sheet and  $\beta$ -turns in water solution. Our experimental findings correlate well with the  $\alpha$ -helical intermediates shown to be important for amyloid formation, especially for the A $\beta$  peptide (Ma & Nussinov, 2006; Murphy & LeVine, 2010; Pike *et al.*, 1993; Klimov & Thirumalai, 2003). Using conformational landscape analysis and molecular dynamics simulations, Ma and Nussinov (2006) investigated the monomeric energy landscape and amyloid formation of the A $\beta$  (25-35) peptide in aqueous solution. They found that the stability of the extended conformation, together with the stability of the  $\alpha$ -helix, is likely to be important for the peptide oligomerization leading to amyloid formation (Ma & Nussinov, 2006). In a recent study of Song *et al.* (2018), FTIR spectra of the peptide in water solution (100  $\mu$ M) after incubation for 12h showed an aggregated  $\beta$ -sheet structure, which is in contrast with our FTIR observations. The incubation time of the peptide sampled in water for 12h may prompt peptides to reach a final equilibrated state at which the aggregated  $\beta$ -sheet structure can appear. In either case, A $\beta$  peptide conformation is critically dependent on the environmental conditions used.

It is pertinent to compare the structure of the aqueous A $\beta$  (25-35) peptide studied here to that of other amyloid peptides. Fonar and Samson (2014) demonstrated by NMR that A $\beta$  (17-34) in water solution adopts an  $\alpha$ -helical structure for the residues 19-26 and 28-33. Another study on a larger peptide, A $\beta$  (1-40) studied in aqueous environment at pH 7.3 using NMR spectroscopy (Vivekanandan *et al.*, 2011) showed that the peptide adopts a stable  $\alpha$ -helical structure in the central hydrophobic core and contacts of the N- and C-termini with the central  $\alpha$ -helix.

As cited above, the  $\alpha$ -helical conformation was detected previously as an intermediate in A $\beta$ -amyloid fibril assembly (Ma & Nussinov, 2006; Fezoui & Teplow, 2002; Kirkitadze *et al.*, 2001; Vivekanandan *et al.*, 2011). It is thus likely that the folding of the A $\beta$  (25-35) monomer as an  $\alpha$ -helical structure is necessary to facilitate the A $\beta$  intermolecular packing within A $\beta$  oligomers. An intramolecular  $\alpha$ -helix formation may occur as a natural consequence of the conformational space by the A $\beta$  (25-35) monomer. Once formed, the intermolecular interactions among these helices containing A $\beta$  monomers could lead to peptide oligomerization followed by a conformational reorganization to form the extended  $\beta$ -sheets that compose the mature amyloid fibril.

This mechanism is supported by previous studies of the fibrillogenesis of A $\beta$  peptides associated with familial forms of cerebral amyloid angiopathy (Kirkitadze *et*

*al.*, 2001) and has been shown to occur in the fibrillogenesis of the model peptide helix-turn-helix (Fezoui *et al.*, 2000; McLaurin *et al.*, 1999). While the  $\alpha$ -helical component in the monomeric structure of the A $\beta$  (25-35) peptide in aqueous solvent seem to play a role in initiating aggregation, the  $\beta$ -turn seen in our experimental and theoretical data may be responsible for the toxicity induced by the soluble monomeric form of this peptide. Indeed, soluble A $\beta$  (25-35) is known to bind to protein receptors on microglia (Doens *et al.*, 2014), leading to their activation and to a subsequent neuronal damage.  $\beta$ -turns are a structural motif often involved in binding to receptor proteins and it is possible that the presence of such turns in A $\beta$  (25-35) may be necessary to induce toxicity (Hashioka *et al.*, 2005).

## 5. Conclusion

Our results show us that A $\beta$  (25-35) in aqueous solution was mostly organized into a  $\alpha$ -helical structure (48%). The contribution of the unordered structure was found to be about 12%. The proportion of  $\beta$ -sheet and  $\beta$ -turn structures are slightly lower, 12-15% and 13-14%, respectively for both concentrations. FTIR spectra of the peptide in water solution (100  $\mu$ M) after incubation for 12h showed A $\beta$  peptide conformation is critically dependent on the environmental conditions used. While the mechanism of toxicity of A $\beta$  (25-35) is still unclear, its native folded structure in aqueous environment is expected to play a role in the aggregation cascade.

### Funding

We are grateful to the Erasmus+, CNRS and the University of Strasbourg for continuous support.

### Conflicts of interest

The authors declare that they have no known competing financial interests or personal relationships that could have appeared to influence the work reported in this paper.

### Availability of data and material

The authors confirm that the data supporting the findings of this study are available within the article and its supplementary materials.

### References

- Barth, A., Zscherp, C. (2002). What vibrations tell about proteins? *Quarterly reviews of Biophysics*, 35(4), 369-430.
- Berthelot, K., Immel, F., Géan, J., Lecomte, S., Oda, R., Kauffmann, B. & Cullin, C. (2009). Driving amyloid toxicity in a yeast model by structural changes: A molecular approach. *The FASEB Journal*, 23(7), 2254-2263.
- Celej, M.S., Sarroukh, R., Goormaghtigh, E., Fidelio, G.D., Ruyschaert, J.M. & Raussens, V. (2012). Toxic prefibrillar  $\alpha$ -synuclein amyloid oligomers adopt a distinctive antiparallel  $\beta$ -sheet structure. *Biochemical Journal*, 443(3), 719-726.



- Cerf, E., Sarroukh, R., Tamamizu-Kato, S., Breydo, L., Derclaye, S., Dufrêne, Y.F. & Raussens, V. (2009). Antiparallel  $\beta$ -sheet: A signature structure of the oligomeric amyloid  $\beta$ -peptide. *Biochemical Journal*, 421(3), 415-423.
- Clementi, M.E., Marini, S., Coletta, M., Orsini, F., Giardina, B. & Misiti, F. (2005). A $\beta$  (31–35) and A $\beta$  (25–35) fragments of amyloid beta-protein induce cellular death through apoptotic signals: Role of the redox state of methionine-35. *FEBS letters*, 579(13), 2913-2918.
- Coles, M., Bicknell, W., Watson, A.A., Fairlie, D.P. & Craik, D.J. (1998). Solution structure of amyloid  $\beta$ -peptide (1–40) in a water–micelle environment. Is the membrane-spanning domain where we think it is? *Biochemistry*, 37(31), 11064-11077.
- D'Errico, G., Vitiello, G., Ortona, O., Tedeschi, A., Ramunno, A. & D'Ursi, A.M. (2008). Interaction between Alzheimer's A $\beta$  (25–35) peptide and phospholipid bilayers: The role of cholesterol. *Biochimica et Biophysica Acta (BBA)-Biomembranes*, 1778(12), 2710-2716.
- Doens, D., Fernández, P. L. (2014). Microglia receptors and their implications in the response to amyloid  $\beta$  for Alzheimer's disease pathogenesis. *Journal of Neuroinflammation*, 11, 1-14.
- D'Ursi, A.M., Armenante, M.R., Guerrini, R., Salvadori, S., Sorrentino, G. & Picone, D. (2004). Solution structure of amyloid  $\beta$ -peptide (25–35) in different media. *Journal of Medicinal Chemistry*, 47(17), 4231-4238.
- El-Agnaf, O.M., Irvine, G.B., Fitzpatrick, G., Glass, W.K. & Guthrie, D.J. (1998). Comparative studies on peptides representing the so-called tachykinin-like region of the Alzheimer A $\beta$  peptide [A $\beta$  (25–35)]. *Biochemical Journal*, 336(2), 419-427.
- Fezoui, Y., Hartley, D.M., Walsh, D.M., Selkoe, D.J., Osterhout, J.J. & Teplow, D.B. (2000). A de novo designed helix-turn-helix peptide forms nontoxic amyloid fibrils. *Nature Structural Biology*, 7(12), 1095-1099.
- Fezoui, Y., Teplow, D.B. (2002). Kinetic studies of amyloid  $\beta$ -protein fibril assembly: Differential effects of  $\alpha$ -helix stabilization. *Journal of Biological Chemistry*, 277(40), 36948-36954.
- Fonar, G., Samson, A.O. (2014). NMR structure of the water soluble A $\beta$ 17–34 peptide. *Bioscience Reports*, 34(6), e00155.
- Hashioka, S., Monji, A., Ueda, T., Kanba, S. & Nakanishi, H. (2005). Amyloid- $\beta$  fibril formation is not necessarily required for microglial activation by the peptides. *Neurochemistry International*, 47(5), 369-376.
- Kirkitadze, M.D., Condrón, M.M. & Teplow, D.B. (2001). Identification and characterization of key kinetic intermediates in amyloid  $\beta$ -protein fibrillogenesis. *Journal of Molecular Biology*, 312(5), 1103-1119.
- Klimov, D.K., Thirumalai, D. (2003). Dissecting the assembly of A $\beta$ 16–22 amyloid peptides into antiparallel  $\beta$  sheets. *Structure*, 11(3), 295-307.
- Kohn, T., Kobayashi, K., Maeda, T., Sato, K. & Takashima, A. (1996). Three-dimensional structures of the amyloid  $\beta$  peptide (25–35) in membrane-mimicking environment. *Biochemistry*, 35(50), 16094-16104.
- Lee, S.W., Kim, Y.M. (2004). Molecular dynamics simulations on  $\beta$  amyloid peptide (25-35) in aqueous trifluoroethanol solution. *Bulletin of the Korean Chemical Society*, 25(6), 838-842.
- Limón, I.D., Díaz, A., Mendieta, L., Chamorro, G., Espinosa, B., Zenteno, E. & Guevara, J. (2009). Amyloid- $\beta$ 25–35 impairs memory and increases NO in the temporal cortex of rats. *Neuroscience Research*, 63(2), 129-137.
- Ma, B., Nussinov, R. (2006). The stability of monomeric intermediates controls amyloid formation: A $\beta$ 25–35 and its N27Q mutant. *Biophysical Journal*, 90(10), 3365-3374.
- McLaurin, J., Franklin, T., Zhang, X., Deng, J. & Fraser, P.E. (1999). Interactions of Alzheimer amyloid- $\beta$  peptides with glycosaminoglycans: Effects on fibril nucleation and growth. *European Journal of Biochemistry*, 266(3), 1101-1110.

- Millucci, L., Ghezzi, L., Bernardini, G. & Santucci, A. (2010). Conformations and biological activities of amyloid beta peptide 25-35. *Current Protein and Peptide Science*, 11(1), 54-67.
- Murphy, M.P., LeVine, III.H. (2010). Alzheimer's disease and the amyloid- $\beta$  peptide. *Journal of Alzheimer's Disease*, 19(1), 311-323.
- Pike, C.J., Burdick, D., Walencewicz, A.J., Glabe, C.G. & Cotman, C.W. (1993). Neurodegeneration induced by beta-amyloid peptides in vitro: The role of peptide assembly state. *Journal of Neuroscience*, 13(4), 1676-1687.
- Resende, R., Pereira, C., Agostinho, P., Vieira, A.P., Malva, J.O. & Oliveira, C.R. (2007). Susceptibility of hippocampal neurons to A $\beta$  peptide toxicity is associated with perturbation of Ca<sup>2+</sup> homeostasis. *Brain Research*, 1143, 11-21.
- Sarroukh, R., Cerf, E., Derclaye, S., Dufrene, Y.F., Goormaghtigh, E., Ruyschaert, J.M. & Raussens, V. (2011). Transformation of amyloid  $\beta$  (1-40) oligomers into fibrils is characterized by a major change in secondary structure. *Cellular and Molecular Life Sciences*, 68, 1429-1438.
- Sarroukh, R., Goormaghtigh, E., Ruyschaert, J.M. & Raussens, V. (2013). ATR-FTIR: A "rejuvenated" tool to investigate amyloid proteins. *Biochimica et Biophysica Acta (BBA)-Biomembranes*, 1828(10), 2328-2338.
- Shanmugam, G., Jayakumar, R. (2004). Structural analysis of amyloid  $\beta$  peptide fragment (25-35) in different microenvironments. *Peptide Science: Original Research on Biomolecules*, 76(5), 421-434.
- Shanmugam, G., Polavarapu, P. L. (2004). Structure of A $\beta$  (25-35) peptide in different environments. *Biophysical Journal*, 87(1), 622-630.
- Song, Y., Li, P., Liu, L., Bortolini, C. & Dong, M. (2018). Nanostructural differentiation and toxicity of amyloid- $\beta$ 25-35 aggregates ensue from distinct secondary conformation. *Scientific Reports*, 8(1), 765.
- Sultana, R., Poon, H.F., Cai, J., Pierce, W.M., Merchant, M., Klein, J.B. & Butterfield, D.A. (2006). Identification of nitrated proteins in Alzheimer's disease brain using a redox proteomics approach. *Neurobiology of Disease*, 22(1), 76-87.
- Terzi, E., Hoelzemann, G. & Seelig, J. (1994). Reversible Random Coil-beta-Sheet Transition of the Alzheimer beta-Amyloid Fragment (25-35). *Biochemistry*, 33(6), 1345-1350.
- Vivekanandan, S., Brender, J.R., Lee, S.Y. & Ramamoorthy, A. (2011). A partially folded structure of amyloid-beta (1-40) in an aqueous environment. *Biochemical and Biophysical Research Communications*, 411(2), 312-316.
- Wei, G., Shea, J.E. (2006). Effects of solvent on the structure of the Alzheimer amyloid- $\beta$  (25-35) peptide. *Biophysical Journal*, 91(5), 1638-1647.
- Zhao, L.N., Lu, L., Chew, L.Y. & Mu, Y. (2014). Alzheimer's disease - A panorama glimpse. *International Journal of Molecular Sciences*, 15(7), 12631-12650.